J Bioenerg Biomembr (2011) 43:187–193
DOI 10.1007/s10863-011-9342-y

NMR solution structure of subunit E (fragment $E_{1–69}$) of the *Saccharomyces cerevisiae* V_1V_O ATPase

Sankaranarayanan Rishikesan · Youg R. Thaker · Gerhard Grüber

Received: 18 November 2010 / Accepted: 31 January 2011 / Published online: 12 March 2011

Abstract The N-terminus of V-ATPase subunit E has been shown to associate with the subunits C, G and H, respectively. To understand the assembly of E with its neighboring subunits as well as its N-terminal structure, the N-terminal region, E_{1-69}, of the *Saccharomyces cerevisiae* V-ATPase subunit E was expressed and purified. The solution structure of E_{1-69} was determined by NMR spectroscopy. The protein is 90.3 Å in length and forms an á-helix between the residues 12–68. The molecule is amphipathic with hydrophobic residues at the N-terminus, predicted to interact with subunit C. The polar epitopes of $E_{1–69}$ are discussed as areas interacting with subunits G and H.

Keywords Vacuolar-type ATPase · V_1V_O ATPase · V-ATPase · Subunit E · Vma4p · *Saccharomyces cerevisiae* · NMR

Abbreviations

DTT	dithiothreitol
EDTA	ethylenediaminetetraacetic acid
IPTG	isopropyl-β-D-thio-galactoside
PMSF	phenylmethylsulfonyl fluoride
Pefabloc^{Sc}	4-(2-Aminoethyl)-benzenesulfonyl fluoride hydrochloride
NMR	nuclear magnetic resonance
NOE	nuclear Overhauser effect
NOESY	NOE spectroscopy
NTA	nitrilotriacetic acid
PAGE	polyacrylamide gel electrophoresis
PCR	polymerase chain reaction
RMSD	root mean square distance
SDS	sodium dodecyl sulfate
Tris	Tris-(hydroxymethyl) aminomethane

S. Rishikesan · Y. R. Thaker · G. Grüber (✉)
School of Biological Sciences,
Nanyang Technological University,
60 Nanyang Drive,
Singapore 637551, Republic of Singapore
e-mail: ggrueber@ntu.edu.sg

Introduction

The proton pump V_1V_O ATPase (V-ATPase) is bound to the membrane of organelles of biosynthetic and endocytic pathways and mediates intra luminal acidification in an ATP-dependent manner, thereby regulating vacuolar protein turnover, vesicular trafficking and vacuolar fusion (Toei et al. 2010). The enzyme also plays a part in the signal transduction processes, which regulate cell growth and survival (Li et al. 2006; Yan et al. 2009) and has been identified as an activator of protein kinase A in response to glucose (Dechant et al. 2010). The enzyme consists of a V_1 ATPase and a membrane-bound sector, V_O. Under certain physiological conditions both sectors can undergo a reversible disassembly (Beyenbach and Wieczorek 2006). ATP is cleaved on the V_1 headpiece consisting of an A_3:B_3 hexamer, and the energy released during that process is transmitted to V_O, to drive the H^+-translocation (Toei et al. 2010; Beyenbach and Wieczorek 2006). This energy-connection occurs via the stalk sector, an assembly of the V_1 and V_O subunits C-H and *a* and *d*, respectively, that form the functional and structural link. The V_O part consists of five different subunits in a stoichiometry of a_1:d_1:c_{4-5}:c'_1:c''_1. The proposed subunit composition and stoichiometry of V_1 is A_3:B_3:C_1:D_1:E_x:F_1:G_y:H_z (Lolkema et al. 2002; Grüber and Marshanski 2008). The stalk subunits of the eukaryotic V_1 ATPase solved so far at high resolution are subunit C (Drory et al. 2004), G (Rishikesan et al. 2009; 2010) and H

(Sagermann et al. 2001) from *Saccharomyces cerevisiae*. Subunit C is formed by an upper head domain, a large globular foot and an elongated neck domain (Drory et al. 2004). The elongated subunit G is mainly α-helical (Rishikesan et al. 2009; 2010), whereby stalk subunit H is characterized by a large, primarily α-helical N-terminal domain, forming a shallow groove, and a C-terminal domain, connected by a four-residue loop (Sagermann et al. 2001).

Subunits H and G can be crosslinked with stalk subunit E, respectively, in the disassembled V_1 ATPase (Xu et al. 1999; Grüber et al. 2000), whereas subunit C is in close proximity to subunit E in both the V_1 sector and the V_1V_O ATPase (Xu et al. 1999; Jones et al. 2005). The E-C assembly is caused by the first 19 N-terminal residues of subunit E which interact with subunit C (Jones et al. 2005). Deletion of the 78 amino terminal residues of subunit E showed that this N-terminal segment is essential for E-H association. Disruption of the E-H subunit interaction resulted in a decrease of both ATP hydrolysis and proton transport activities of *Saccharomyces cerevisiae* V-ATPase (Lu et al. 2002). Besides its physical association with V-ATPase subunits, E interacts also with regulatory proteins like the Dbl homology domain of the guanine nucleotide exchange factor mSOS, linking V-ATPase with the small G protein Rac1 (Lu et al. 2001). In human kidney, subunit E of V-ATPase assembles directly with the glycolytic enzyme aldolase, thereby providing a coupling mechanism with the glycolytic pathway (Lu et al. 2001; Miura et al. 2001).

Subunit E is predicted to contain an N-terminal extended α helix with a C-terminal part, consisting of a mixture of α-helices and β-sheet structures (Jones et al. 2005). Because of the central role of subunit E and the critical role of its N-terminus in subunit-subunit interaction, knowledge about its structural details is essential. Here we describe the production, purification and structural studies of the N-terminal region of subunit E of the V-ATPase from *S. cerevisiae*, $E_{1–69}$, in solution using nuclear magnetic resonance spectroscopy. Based on the $E_{1–69}$ structure the residues involved in E-C, E-G and E-H assembly are discussed.

Materials and methods

Biochemicals

ProofStart™ DNA Polymerase and Ni^{2+}-NTA-chromatography resin were received from Qiagen (Hilden, Germany); restriction enzymes were purchased from Fermentas (St. Leon-Rot, Germany). Chemicals for gel electrophoresis were received from Serva (Heidelberg, Germany). ($^{15}NH_4$)Cl and (^{13}C) glucose were purchased from Cambridge Isotope Laboratories (Andover, U.S.A.). All other chemicals were at least of analytical grade and received from BIOMOL (Hamburg, Germany), Merck (Darmstadt, Germany), Sigma (Deisenhofen, Germany), or Serva (Heidelberg, Germany).

Expression and purification of recombinant E_{1-69}

$E_{1–69}$ was cloned from the *S. cerevisiae* genome through the PCR cloning method using 5'-TTT-CCA-TGG-CCT-CCG-CTA-TTA-CTG-3' as forward primer and 5'-CTA-TGA-GCT-CTC-ATG-CCT-TCT-TCA-ACT-TG-3' as reverse primer. PCR products incorporating NcoI and SacI restriction sites were digested and ligated to the pET9d(+)-His_3 vector (Grüber et al. 2002). The uniformly ^{15}N- and $^{15}N/^{13}C$- labeled E_{1-69} was expressed in *Escherichia coli* BL21 (DE3) cells using M9 minimal media containing $^{15}NH_4Cl$, or $^{15}NH_4Cl$ plus [U-^{13}C]-glucose. To induce production of proteins, cultures were supplemented with isopropyl-β-D-thio-galactoside (IPTG) to a final concentration of 1 mM. Cells were harvested at 8 000 x g for 15 min at 4°C and lysed on ice by sonication for 3×1 min at 50% power in the buffer (50 mM HEPES, pH 7.0, 200 mM NaCl, 1 mM DTT, 2 mM 4-(2-Aminoethyl)-benzenesulfonyl fluoride hydrochloride (Pefabloc^{Sc}) and 2 mM phenylmethylsulfonyl fluoride (PMSF). The lysate was cleared by centrifugation at 10 000 x g for 30 min at 4°C, and the supernatant was passed through a filter (0.45 mm pore-size) supplemented with Ni^{2+}-NTA resin. The N-terminal His-tagged protein, (MKHHH-E_{1-69}), was allowed to bind to the matrix for 2 h at 4°C by mixing on a sample rotator (Neolab), and eluted with an imidazole-gradient (25–250 mM) in the buffer described above. Fractions containing His-tagged proteins were identified by SDS-PAGE (Laemmli 1970), pooled and concentrated using Centriprep YM-3 (3 kDa molecular mass cut-off) spin concentrators (Millipore) and subsequently applied on a size exclusion column Superdex HR75 (10/30, GE Healthcare). Selected fractions were concentrated in 3 kDa cut-off centricon. The purity of the protein sample was analyzed by SDS-PAGE. The SDS-gels were stained with Coomassie Brilliant Blue R250. Protein concentrations were determined by the bicinchoninic acid assay (BCA; Pierce, Rockford, IL, USA).

CD spectroscopy of *S. cerevisiae* $E_{1–69}$

Circular dichroism (CD) spectra of $E_{1–69}$ were measured in the far UV-light (190–260 nm) using a CHIRASCAN spectrometer (Applied Photophysics). Spectra were collected in a 60 µl quartz cell (Hellma) with a path length of 0.1 mm, at 20°C at a step resolution of 1 nm. The readings were average of 2 s at each wavelength and the recorded millidegree values were the average of three determinations for the sample. The CD spectrum was acquired in a buffer of

25 mM phosphate (pH 6.8), 200 mM NaCl and 5 mM EDTA with a protein concentration of 2.0 mg/ml (0.25 mM). The spectrum of the buffer was subtracted from the spectrum of $E_{1–69}$. CD values were converted to mean residue molar ellipticity (θ) in units of deg × cm^2 × $dmol^{-1}$ x aa^{-1} using the software C*hirascan Version 1.2*, Applied Photophysics. This baseline corrected spectrum was used as input for computer methods to obtain predictions of secondary structure.

NMR data collection and processing

The NMR sample, 1 mM of $E_{1–69}$, was prepared in 90% H_2O and 10% D_2O containing 25 mM NaH_2PO_4 (pH 6.8), 200 mM NaCl and 5 mM EDTA. All NMR experiments were performed at 288 K on a Bruker Avance 600 MHz spectrometer. The experiments recorded on $^{15}N/^{13}C$-labelled sample were HNCO, CBCA(CO)NH, HNCACB and 3D ^{15}N-NOESY-HSQC. The 3D ^{15}N-NOESY-HSQC was recorded using a mixing time of 200 ms. All the two- and three-dimensional experiments made use of pulsed-field gradients for coherence selection and artifact suppression, and utilized gradient sensitivity enhancement schemes. Quadrature detection in the indirectly detected dimensions was achieved using either the States/TPPI (time-proportional phase incrementation) (Marion et al. 1989) or the echo/anti-echo method (Bax et al. 1980; Claridge 1999). Baseline corrections were applied wherever necessary. The proton chemical shift was referenced to the methyl signal of DSS (2, 2-dimethyl-2-silapentane-5-sulphonate (Cambridge Isotope Laboratories) as an external reference to 0 ppm. The ^{13}C and ^{15}N chemical shifts were referenced indirectly to DSS. All the NMR data were processed using Bruker Avance spectrometer in-built software Topspin 2.1 version. Peak-picking and data analysis of the Fourier transformed spectra were performed with the SPARKY program (Kneller and Goddard 1997).

NMR spectroscopy and structure calculation of $E_{1–69}$

The additional His-residues of the His-tag at the N-terminus of $E_{1–69}$, which are essentially unstructured, were not used in the structure calculation. The structure calculation was performed from the first methionine in the N-terminal which is after the proline residue. The sequential assignments were achieved using triple-resonance backbone experiments (HNCO, CBCA(CO)NH and HNCACB) and all the side chain assignments were done using the (H) CCCONH experiment. Dihedral angle restraints were calculated from Cα and Cβ chemical shifts by using PREDITOR (Berjanskii et al. 2006). The distance constraints for the structure calculation were collected from 3D ^{1}H-^{15}N NOESY-HSQC by manually and automatically assigned NOE using CYANA 3.0 (Wüthrich 1986; Herrmann et al. 2002). Seven cycles of automated NOESY assignment using the CYANA 3.0 package were performed. In the final CYANA cycle NOESY cross peaks were assigned unambiguously, leading to 921 meaningful NOE distance restraints. 10 conformers of the monomeric $E_{1–69}$ were calculated based on the obtained dihedral angles and NOE restraints. The program MOLMOL was used to visualize the result of ensemble of minimized conformers (Koradi et al. 1996). The coordinates for the structure of $E_{1–69}$ have been deposited in the Protein Data Bank with code 2KZ9.

Results and discussion

Protein production and purification of $E_{1–69}$

Subunit E of the V-ATPase from *S. cerevisiae* is composed of 233 amino acids, divided into a predicted α-helix at the N-terminal part and an α-helical and β-sheet containing domain at the C-terminus (Jones et al. 2005; Grüber et al. 2002). As the N-terminal segment of subunit E has been shown to play an important role in the assembly of V-ATPase subunits, by interacting with subunits C, G and H, the construct $E_{1–69}$, containing the N-terminal 69 residues, was designed for NMR structural studies. The SDS-PAGE of the recombinant *S. cerevisiae* $E_{1–69}$ revealed a prominent band of about 7.9 kDa, which was found within the soluble fractions. A Ni^{2+}-NTA resin column and an imidazole-gradient (25–250 mM) in 50 mM HEPES, pH 7.0, 200 mM NaCl, 1 mM DTT, 2 mM Pefabloc^{SC} and 2 mM PMSF was used to purify the protein. The elution fractions from the Ni^{2+}-NTA purification containing the E_{1-69} were collected and applied on to a size exclusion column. Analysis of the isolated protein by SDS-PAGE revealed a high purity of $E_{1–69}$ (Fig. 1a). The secondary structure of $E_{1–69}$ was determined from circular dichroism spectra that were measured between 190–260 nm (Fig. 1b). The minima at 222 and 208 nm and the maximum at 192 nm indicate the presence of α-helical structures in the protein. The average secondary structure content was 81±4% α-helix and 19± 3% random coil.

Resonance assignment of *S. cerevisiae* $E_{1–69}$

Assignment for the backbone HN, N, Cα, Cβ, and C' resonance of $E_{1–69}$ was achieved by a combined analysis of the triple resonance HNCACB, CBCA(CO)NH and HNCO spectra. Figure 2a shows the good quality of the assigned HSQC spectrum indicating backbone HN and ^{15}N cross peaks of all the residues of $E_{1–69}$. Overall, the limited chemical shift dispersion of around ~2.0 ppm for the amide proton resonance together with the appropriate medium-

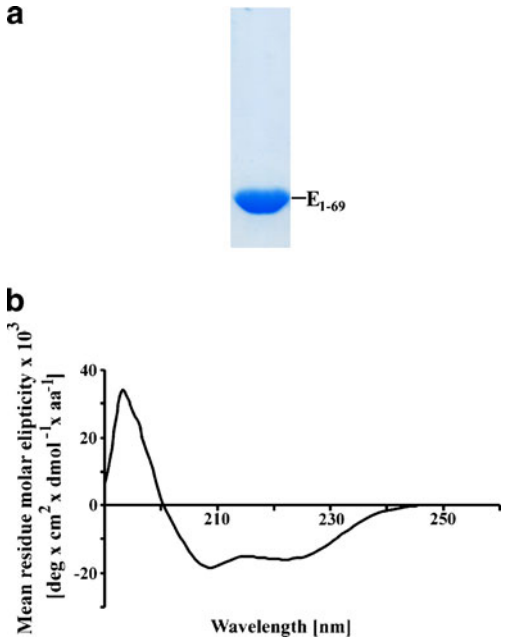

Fig. 1 **a** SDS gel (17% total acrylamide and 0.4% crosslinked acrylamide) of the recombinant $E_{1–69}$ of the *S. cerevisiae* V-ATPase and **b** Far UV-CD spectrum of $E_{1–69}$

range NOEs (Fig. 2b) indicates a predominantly helical protein (Wüthrich et al. 1982).

NMR derived 3-dimensional structure of *S. cerevisiae* $E_{1–69}$

Two- and three dimensional NMR experiments were performed to observe the solution structure of $E_{1–69}$. The structure of $E_{1–69}$ was calculated on the basis of a total 921 nontrivial NMR-derived distance restraints (284 were intraresidual, 304 were sequential and 160 were medium range) through molecular dynamics and simulated annealing (Table 1). Hydrogen bonds were identified from the characteristic patterns of homonuclear ^1H nuclear Overhausser enhancements (NOEs) (Wüthrich et al. 1982) and were introduced at the end of structure calculations. Typical α-helical NOE pattern $d_{\alpha N}$ (i, i+3), $d_{\alpha N}$ (i, i+4) and $d_{\alpha\beta}$ (i, i+3) were observed from the amino acid residues 12 to 68. A bar diagram summarizing the backbone and the backbone/sidechain NOE connectivities of $E_{1–69}$ is illustrated in Fig. 2b. The statistics of the 10 lowest energy structures of $E_{1–69}$ are described in the table 1. These 10 structures have an overall RMSD of 0.59 Å for the backbone atoms and 1.70 Å for all the heavy atoms in the helical region of the three dimensional structures (residue 12–68) of the peptide. All these structures have energies lower than 4 kcal/mol, no NOE violations greater than 0.3 Å, and no dihedral violations greater than 5°. Analysis of the Ramachandran plot for the calculated structure shows 87.9% residues in the most favored regions and 12.1% of the residues in the additionally allowed regions. As shown in Fig. 3a, $E_{1–69}$ has an extended helical structure from the residues Gln12 to Lys68 measuring a length of 83.19 Å, as predicted from the amino acid sequence and the secondary structure prediction of $E_{1–69}$. The peptide consists of 34.8% charged residues, 27.5% other polar residues and 37.7% non-polar residues in the sequence. The solution structure illustrates a clear amphipathic helix with a hydrophobic N-terminus on one side of the helix and a highly charged C-terminus, exposing the charged residues

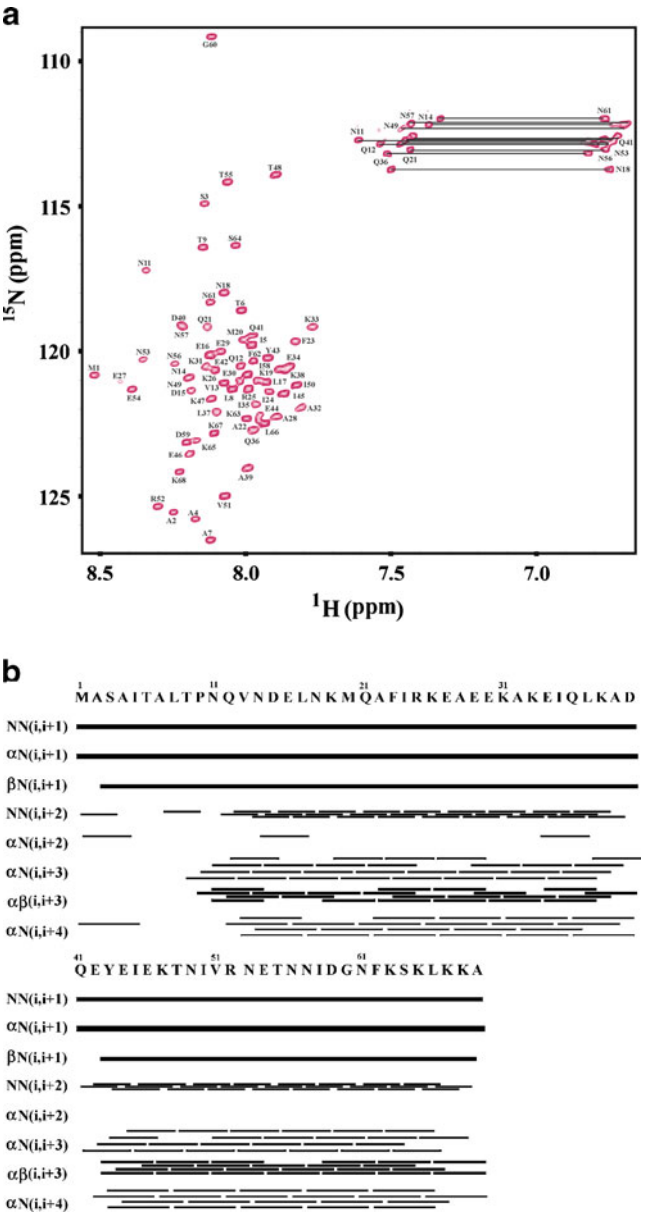

Fig. 2 **a** 2D ^1H-^{15}N-HSQC spectrum of *S. cerevisiae* $E_{1–69}$ (1 mM) in 25 mM sodium phosphate buffer (7.0), 200 mM NaCl and 5 mM EDTA at 288 K. Signals from the side-chain NH_2 groups are connected by horizontal lines. **b** The NOESY connectivity plot of $E_{1–69}$ indicative of the residues connected in space revealing the presence of helical structure

Table 1 Statistics for the 10 selected structures of $E_{1–69}$ of the *S. cerevisiae* V-ATPase

Total Number of NMR restraints	921
Number of unambiguous NOE peaks	
Intraresidual (|i-j|=0)	284
Sequential (|i-j|=1)	304
Meduim-range (2≤|i-j|≤5)	160
Long-range (|i-j|>5)	0
Number of Dihedral angle constraints	118
Number of hydrogen-bond distance restraints	55
Number of restraint violations	
Total number of restraint violations>0.3 Å	0
Total number of dihedral angle violations>5°	0
Ramachandran Plot Statistics (%)	
Fractions of residues of most favoured regions (%)	87.9
Fractions of residues in additionally allowed regions (%)	12.1
Fractions of residues in generously allowed regions (%)	0
Fractions of residues in disallowed regions (%)	0
Structural precision of well ordered region	
RMSD backbone (residues (12–68)	0.59 Å
RMSD heavy (residues 12–68)	1.70 Å

towards the outer surface of the structure (Fig. 3b). Most recently, the crystallographic structure of the related subunit E, including the residues 2 to 94, of the *Thermus thermophilus* A_1A_O ATP synthase has been solved (Lee et al. 2010) (Fig. 4). When positioned inside the crystallographic structure of $E_{2–94}$ the NMR structure of $E_{1–69}$ accommodated very well, with R.M.S.D. values of 1.481 for residues Phe23-Ala69 ($E_{1–69}$) and residues Ser29-Ala75 ($E_{2–94}$) (Fig. 4), thereby confirming the α-helical feature determined for the *S. cerevisiae* $E_{1–69}$.

Interaction of subunit E with its neighboring subunits C, G and H

Like the stalk subunit G, E has been reported to be present in multiple copies of the eukaryotic V-ATPase (Kitagawa et al. 2008), enabling its interaction with multiple stalk subunits within the enzyme complex. Biochemical data with truncated forms of subunit E of the *S. cerevisiae* V-ATPase have shown that deletions of the N-terminal 38 residues ($E_{39–233}$) results in a complete loss of E-G association. More recently, NMR titration experiments using the recombinant yeast $G_{1–59}$ and the subunit E peptide, $E_{18–38}$, residues Val22, Ser23, Lys24, Ala25 and Arg26 of subunit G as well as amino acids Met20, Glu29 and Glu30 of $E_{18–38}$ could be described as being involved in the E-G assembly (Rishikesan et al. 2008). The present NMR structure of $E_{1–69}$ reveals that the side, including the residues Met20, Glu29 and Glu30, is enriched in charged residues of which 10 are almost universally conserved among eukaryotic V-ATPases (Fig. 3c). Together with the high portion of charged residues in subunit G, the polar surfaces of E and G may form the interacting area of both stalk subunits as predicted from site directed mutagenesis of the yeast G subunit (Charsky et al. 2000).

Whereas the deletion of the N-terminal 19 amino acids does not affect the E-G interaction, the association of C and E are significantly reduced after removal of the first 19 amino acids of subunit E of the V-ATPase from *S. cerevisiae* (Jones et al. 2005), suggesting that the regions at the N-terminus of subunit E discriminates between

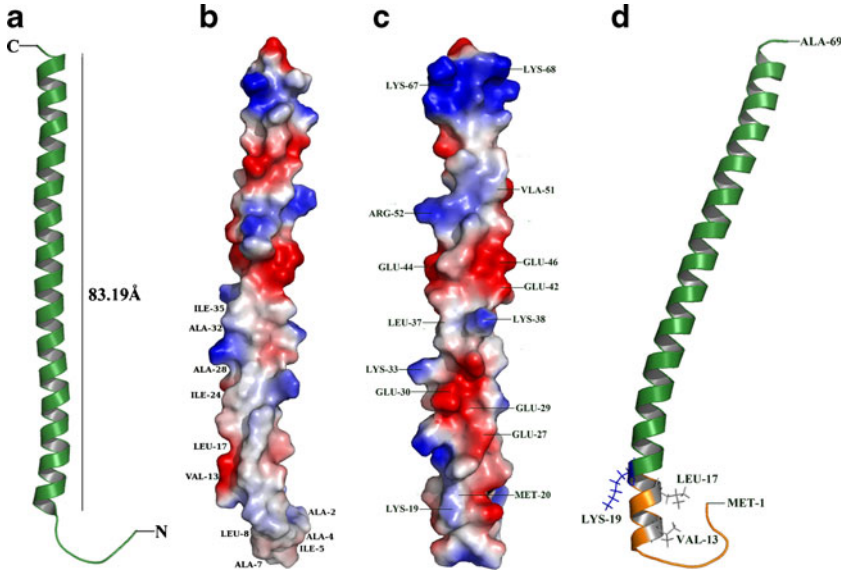

Fig. 3 NMR solution structure of *S. cerevisiae* $E_{1–69}$. **a** Side view of the average structure of $E_{1–69}$. **b-c** Orientation of $E_{1–69}$ showing the molecular surface with the electrostatic potential of the peptide, drawn in PyMol (DeLano 2001), where the positive potentials are drawn in blue, negative in red and hydrophobic surface in white color. **d** Ribbon diagram of $E_{1–69}$ showing the first 19 amino acids in orange. The hydrophobic residues Val13 and Leu17 are highlighted in grey and the positively charged residue Lys19 is shown in blue. These amino acids are described to be important in the C-E assembly (Jones et al. 2005)

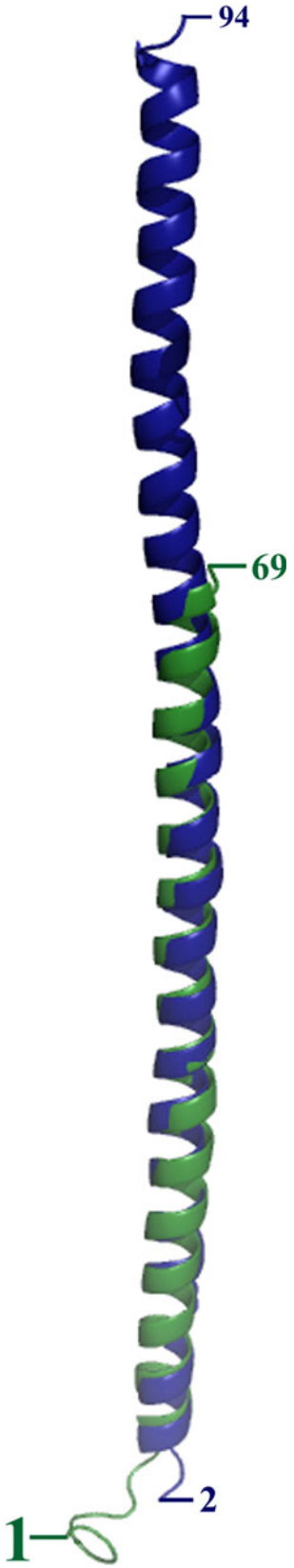

Fig. 4 NMR structure of *S. cerevisiae* $E_{1–69}$ (*green*) from yeast V-ATPase superimposed on to the crystallographic structure of $E_{2–94}$, of the *T. thermophilus* subunit E (*blue* (Lee LK et al. 2010))

binding of subunit C or G. As described by Jones et al. 2005, this very N-terminal segment is missing in the related A_1A_O ATP synthases from archaea, which have no counterpart of the eukaryotic subunit C (Grüber and Marshanski 2008), making this sequence a key determinant in the interaction of subunits C and E in eukaryotic V-ATPases. Mutagenesis studies have shown that the C-E assembly in the *S. cerevisiae* V-ATPase are mediated primarily by hydrophobic residues, like Val13 and Leu17, pointing to the role for hydrophobic interaction in the C-E assembly (Jones et al. 2005). As the NMR solution structure of $E_{1–69}$ shows, both residues are located on one side and would support a hydrophobic interaction of both subunits (Fig. 3d). Interestingly, *in vivo* mutagenesis also demonstrated that single substitutions of the hydrophobic residues Val13 and Leu17 and the positively charged Lys19 on the other side of the helix, respectively, resulted in loss of V-ATPase function (Jones et al. 2005). Subunit C consists of two globular domains, a so-called foot and head domain which are linked via a helical coiled coil region (Drory et al. 2004). From *in vitro* data it has been proposed, that the head region of subunit C would strongly interact with subunit E (Oot and Wilkens 2010). Because of the globular shape of the head region of subunit C, we propose that the very N-terminus of E may become anchored in the globular domain of subunit C, allowing the hydrophobic and polar residues of E to interact with the corresponding amino acids in C.

The third critical partner of subunit E in stalk formations is the 52 kDa subunit H. Removal of 78 residues of the N-terminus of subunit E results in loss of both, E-H assembly and proper V-ATPase function (Lu et al. 2003). At the moment we can only speculate, whether some of the charged residues, distributed on both sides of the $E_{1–69}$ structure (Fig. 3b-c) and attributed by Lys19, Arg25, Lys26, Glu27, Glu29, Glu30, Lys31, Lys33, Glu34, Lys38, Glu42, Glu44, Glu45, Lys46, Arg52, Glu54, Lys63, Lys65, Lys67 and/or Lys68, may be important for its assembly with subunit H (Lu et al. 2002). However, together with the crystallographic structure of *S. cerevisiae* subunit H^{11} the NMR solution structure of $E_{1–69}$ provides the essential information to generate appropriate mutant proteins of subunit E and H to resolve the critical amino acids involved in E-H assembly, which are required for ATPase activity and H^+-pumping (Lu et al. 2002). In addition, *in vivo* studies such E-H mutants will provide insights into the mechanisms that influence this assembly in response to physiological factors such as aldolase-, Db1- or Rac1-binding to subunit E.

Acknowledgment S. Rishikesan and Y. R Thaker are grateful to the authority of Nanyang Technological University (NTU) for awarding research scholarship. This research was supported by A*STAR BMRC (09/1/22/19/609). We thank Dr. S. Gayen (SBS, NTU) for helpful suggestions concerning NMR data analysis and we are grateful to Dr. M. S. S. Manimekalai (SBS, NTU) for reading the manuscript.

References

Charsky CMH, Schumann NJ, Kane PM (2000) J Biol Chem 275:37232–37239

Bax A, Freemna R, Kempsell SP (1980) J Magn Reson 41:349–353

Berjanskii MV, Neal S, Wishart DS (2006) Nucleic Acids Res 34:63–69

Beyenbach KW, Wieczorek H (2006) J Exp Biol 209:577–589

Claridge TDW (1999) High-Resolution NMR technique in organic chemistry

Dechant R, Binda M, Lee SS, Pelet S, Winderick J, Peter M (2010) EMBO J 29:2515–2526

DeLano WL (2001) The pyMol molecular graphics system. DeLano Scientific, San Carlos

Drory O, Frolow F, Nelson N (2004) EMBO Rep 5:1148–1152

Grüber G, Marshanski V (2008) Bioessays 30:1096–1099

Grüber G, Radermacher M, Ruiz T, Godovac-Zimmermann J, Canas B, Kleine-Kohlbrecher D, Huss M, Harvey WR, Wieczorek H (2000) Biochemistry 39:8609–8616

Grüber G, Godovac-Zimmermann J, Link TA, Coskun Ü, Rizzo VF, Betz C, Bailer S (2002) Biochem Biophys Res Comm 298:383–391

Herrmann T, Güntert P, Wüthrich K (2002) J Mol Biol 319:209–227

Jones RPO, Durose LJ, Findlay JBC, Harrison MA (2005) Biochemistry 44:3933–3941

Koradi R, Billeter M, Wüthrich K (1996) J Mol Graph 14:51–55

Kitagawa N, Mazon H, Heck AJR, Wilkens S (2008) J Biol Chem 283:3329–3337

Kneller DG, Goddard TD (1997) SPARKY 3.105. University of California, San Francisco

Laemmli UK (1970) Nature 227:680–685

Lee LK, Stewart AG, Donohoe M, Bernal RA, Stock D (2010) Nature Struct Mol Biol 17:373–378

Li G, Yang Q, Krishnan S, Alexander EA, Borkan SC, Schwartz JH (2006) Cell Death Differ 13:2109–2117

Lolkema JS, Chaban Y, Boekema EJ (2002) J Bioenerg Biomembr 35:323–336

Lu M, Vergara S, Zhang L, Holliday S, Aris J, Gluck SL (2002) J Biol Chem 277:38409–38415

Lu M, Holliday LS, Zhang L, Dunn WA, Gluck SL (2001) J Biol Chem 276:30407–30413

Lu M, Sautin YY, Holliday LS, Zhang L, Dunn WA, Gluck SL (2003) J Biol Chem 279:8732–8739

Marion D, Ikura M, Tschudin R, Bax A (1989) J Magn Reson 85:393–399

Miura K, Miyazawa S, Furuta S, Mitsushita J, Kamijo K, Ishida H, Miki T, Suzukawa K, Resau J, Copeland TD, Kamata T (2001) J Biol Chem 276:46276–46283

Oot RA, Wilkens S (2010) J Biol Chem 285:24654–24664

Rishikesan S, Thaker YR, Priya R, Gayen S, Manimekalai MSS, Hunke C, Grüber G (2008) Mol Membr Biol 25:400–410

Rishikesan S, Gayen S, Thaker YR, Vivekanandan S, Manimekalai MSS, Yau YH, Geifman Shochat S, Grüber G (2009) Biochim Biophys Acta—Bioenergetics 1787:242–251

Rishikesan S, Manimekalai MSS, Grüber G (2010) Biochim Biophys Acta—Biomembranes 1798:1961–8

Sagermann M, Stevens TH, Matthews BW (2001) Proc Natl Acad Sci USA 98:7134–7139

Toei M, Saum R, Forgac M (2010) Biochemistry 49:4715–4723

Wüthrich K (1986) NMR of proteins and nucleic acids. Wiley, New York

Wüthrich K, Wider G, Wagner G, Braun W (1982) J Mol Biol 155:311–319

Xu T, Vasilyeva E, Forgac M (1999) J Biol Chem 274:28909–28915

Yan Y, Denef N, Schupbach T (2009) Dev Cell 17:387–402